sustainability

MDPI

Article

Spatiotemporal Changes and Trade-Offs/Synergies of Waterfront Ecosystem Services Globally

Yaomin Zheng [1,2], Huize Yang [1,2], Huixin Gong [1,2,*], Jinlian Shi [1,2], Yanhui Zhang [1,2], Jiaxin Wang [2], Xin Zhang [1,2], Ruifen Cheng [1,2] and Yu Chen [3,*]

[1] Business School, Beijing Technology and Business University, Beijing 100048, China; 20200901@btbu.edu.cn (Y.Z.); helly_yang0622@163.com (H.Y.)
[2] Institute for Culture and Tourism Development, Beijing Technology and Business University, Beijing 100048, China
[3] Aerospace Information Research Institute, Chinese Academy of Sciences, Beijing 100101, China
* Correspondence: 2231001049@st.btbu.edu.cn (H.G.); chenyu@radi.ac.cn (Y.C.)

Abstract: The types of ecosystem services are complex and diverse. This study estimated four ecosystem services, their trade-offs, and their synergistic outcomes in 2010, 2015, and 2020 using the InVEST model. Globally, results showed that waterfront ecosystem services are high (low) in the north (south), and that high-value areas are mainly in Sweden and Finland in Europe; the Congo in Africa; Russia, Southwest China, and Indonesia in Asia; the Northwestern United States and Canada in North America, and northeastern Peru and northwestern Brazil in South America. Overall, ecosystem services changed little during 2010–2020. Additionally, a notable trade-off was found between water yield and habitat quality, and strong synergies were found between water yield and carbon storage and sequestration, water yield and sediment delivery ratio, carbon storage and sequestration and sediment delivery ratio, and carbon storage and habitat quality. The results of this study could help promote sustainable development of waterfronts globally.

Keywords: waterfront; ecosystem services; InVEST model; sustainable development

check for updates

Academic Editors: Dan Chen, Qiong Yue and Zhaohui Luo

Received: 17 November 2024
Revised: 24 December 2024
Accepted: 8 January 2025
Published: 9 January 2025

Citation: Zheng, Y.; Yang, H.; Gong, H.; Shi, J.; Zhang, Y.; Wang, J.; Zhang, X.; Cheng, R.; Chen, Y. Spatiotemporal Changes and Trade-Offs/Synergies of Waterfront Ecosystem Services Globally. *Sustainability* **2025**, *17*, 472. https://doi.org/10.3390/su17020472

Copyright: © 2025 by the authors. Licensee MDPI, Basel, Switzerland. This article is an open access article distributed under the terms and conditions of the Creative Commons Attribution (CC BY) license (https://creativecommons.org/licenses/by/4.0/).

1. Introduction

The phrase ecosystem services (ESS) refers to the various benefits that humans obtain directly or indirectly from the natural environment. They serve as a bridge between human society and natural ecology and play important roles in improving human well-being, promoting ecological security, and maintaining sustainable economic development [1,2].

According to the 2005 United Nations Millennium Ecosystem Assessment, 60% of ESS globally are degraded, and this proportion is expected to increase further as urbanization accelerates and the intensity of human activities increases [3]. Therefore, it is important to maintain ESS or to slow their degradation to maintain harmony between natural ecosystems and human activities. Consequently, ESS assessment and the study of ESS trade-offs have become important topics of research [4].

The types of ESS are complex and diverse, and multiple ESS might exist concurrently within a region [5]. Different ESS are interrelated, and the nature of their interaction can be complex, e.g., trade-off, synergy, or irrelevance [6,7]. The trade-offs and synergies between ESS are not fixed and will change over time. Therefore, studying the dynamic change mechanism between ESS can provide methodological support for enhancing the synergies and weakening the trade-offs between ESS [5]. Recent studies have examined the trade-offs and synergies between ESS at different scales. For example, Liu et al. [6]

evaluated the spatiotemporal changes and trade-off/synergy relationships among the three ESS of water yield (WY), carbon storage, and soil retention in Beijing (China) in 1984, 1995, 2005, and 2018. Wang et al. [8] investigated the trade-offs and synergies among five ecosystem services, i.e., WY, water purification, carbon storage, soil conservation, and food supply, in the Wulan Su watershed (China) for the years 2000, 2005, 2010, 2015, and 2018, and they considered the impact of land-use type changes on these ESS. Ren et al. [6,8,9] analyzed the trade-offs and synergies between water conservation, carbon storage, soil conservation, and habitat quality (HQ) services during 2000–2020 in the middle reaches of the Yellow River (China). Their results suggested that land-use change is one of the key drivers affecting ESS, and that marked differences exist in spatiotemporal variations in different ESS between land cover types [8,10,11]. Therefore, assessing the impact of land-use change on ESS can help with implementation of appropriate land-use programs and provide scientific support for sustainable development of ESS [12,13]. However, earlier related studies largely evaluated ESS in watersheds, cities, and parks, and few studies have considered the spatiotemporal changes, trade-offs, and synergies of ESS in waterfront environments. Therefore, this study took waterfront environments globally as the research scope for analysis and evaluation [8,14].

The waterfront environment refers to the boundary area between rivers, lakes, oceans, or other water bodies and the surrounding land, which can be both regional infrastructure and regional public space, providing many waterfront ESS of differing values [15–17]. Waterfronts play a vital role in creating jobs, enhancing urban vitality, stimulating commercial activities, and promoting attractiveness for tourism [18–20]. According to preliminary estimates, most leisure and recreation industries globally are concentrated in waterfront areas, accounting for 10.3% of the total global GDP [21]. Additionally, waterfront landscapes are diverse, ecologically sensitive, and economically active, and their functions change according to land-use types [21,22]. Therefore, it is important to evaluate waterfront ESS to raise the conservation awareness of residents and tourists, formulate policies for ecological protection and recreation management of waterfronts, and coordinate sustainable socioeconomic and ecosystem development [23,24].

Based on land-use data from 2010, 2015, and 2020, and combined with meteorological and soil data, this study used the InVEST model to calculate four ESS of waterfronts (i.e., WY, carbon storage and sequestration (CS), soil conservation (i.e., sediment delivery ratio (SDR)), and HQ) in terms of three aspects: comprehensive supply services, regulation services, and support services. The results of the spatiotemporal changes and trade-offs of ESS in waterfronts globally, visualized and analyzed using ArcGIS 10.8 and R Studio software (R 4.4.2), were used to explore the relationship between these four types of ESS and land use. The primary objective of this study was to provide suggestions for sustainable development of waterfronts globally [25,26].

2. Materials and Methods

2.1. Overview of the Study Area

The term waterfront refers to a certain region in an urban area where land and water are connected, representing a mixed zone of aquatic and terrestrial ecologies [27–29]. Despite a lack of consensus among the academic community, the specific spatial scope of the waterfront area is generally considered to vary, owing to different factors such as history and culture, planning structure, degree of development, and natural climate [30]. In this study, different buffer zones were established according to the water system level: the buffer zone was set to the range of 2000 m for water system levels 0 and 1; the buffer zone was set to the range of 2000 m for water system level 2; the buffer zone was set to the range of 500 m for water system level 3; the buffer zone was set to the range of 200 m for

water system level 4; and the buffer zone was set to the range of 100 m for water system level 5. Finally, the waterfront range globally was obtained, as shown in Figure 1.

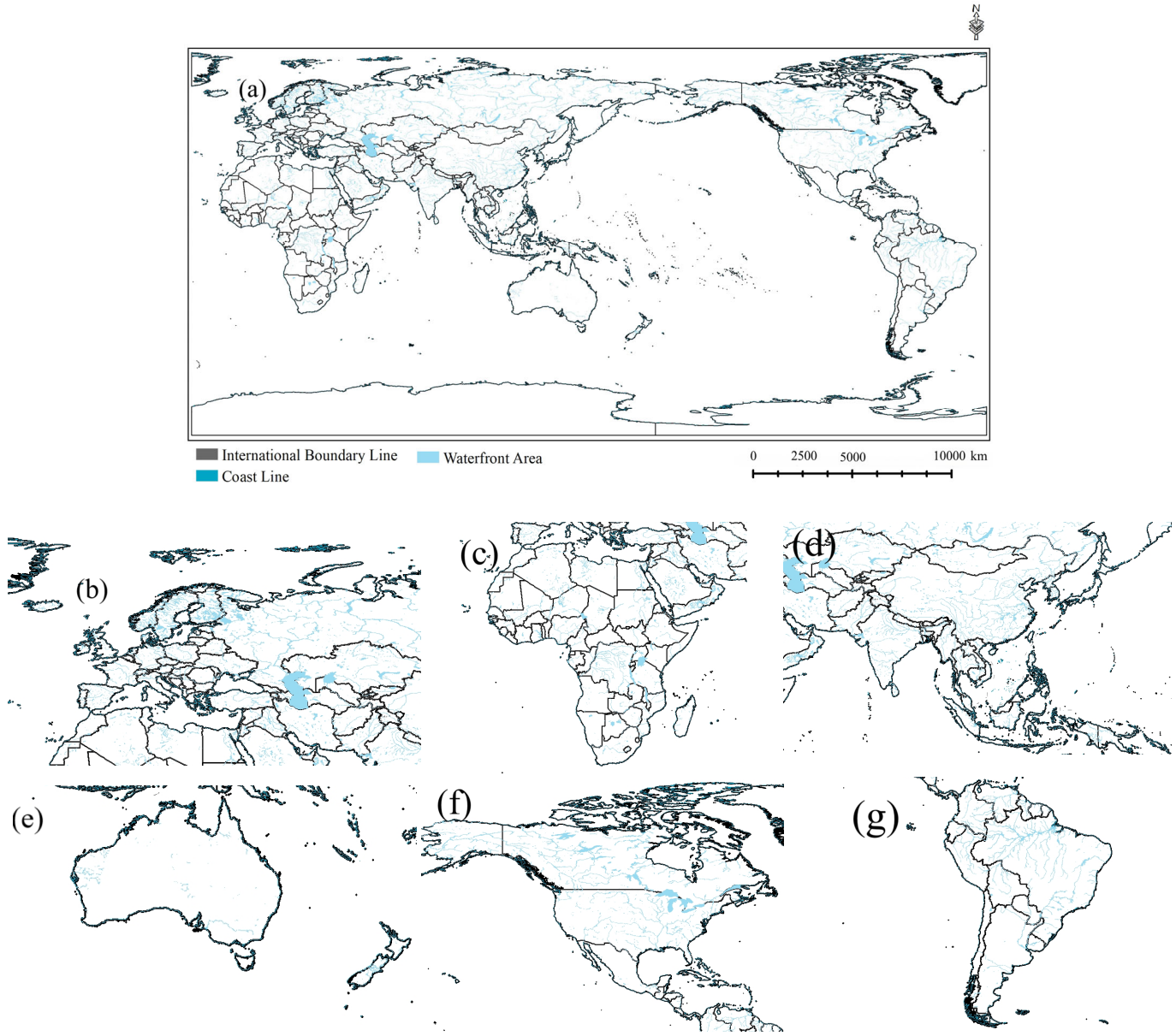

Figure 1. (**a**) Global waterfront extent (global and continental). (**b**): Europe; (**c**): Africa; (**d**): Asia; (**e**): Oceania; (**f**): North America; (**g**): North America.

In 2020, the global waterfront area covered approximately 6,692,500 km^2, with water (38.84%) and forest (27.74%) ranking first and second, respectively, with both exceeding 25% of the total waterfront area. These were followed in descending order by farmland (11.72%), bare land (9.08%), grassland (4.87%), wetland (3.71%), shrub (3.07%), construction land (0.97%), and area of ice and snow (0.01%). During 2010–2020, construction land, wetland, shrub, water, and grassland all showed a trend of increase in area, among which the area of construction land increased the most (by 22.34%), followed by wetlands (by 3.36%). Forest, bare land, and farmland all showed a trend of reduction in area, among which the area of forest decreased the most (by 1.21%), followed by bare land (by 0.47%). The area of ice and snow remained broadly unchanged.

2.2. Research Methodology

This study uses the InVEST model, developed jointly by Stanford University and others in the United States, to innovate and improve the coefficients of the biophysical table, based on which the annual WY, CS, SDR, and HQ of waterfront areas globally in 2010, 2015, and 2020 were analyzed [30–32]. The total supply of global waterfront ESS was obtained by superimposing the equal weights of the four ESS, and the calculation results were visualized and evaluated through GIS spatial analysis.

InVEST allows for the qualification of multiple ecosystem services, such as water filtration, food regulation, habitat provision, and recreational opportunities. It can convert these services into monetary values, facilitating better decision making for related users. So, the model can significantly enhance our understanding of waterfront ecosystems by providing a structured approach to assess, value, and manage ecosystem services [33].

The novelty of this research is as follows: In general, there is an analysis of the situation in the world and China in 2020, and the changes in ESS are selected in 2020, 2015, and 2020.

2.2.1. Water Yield Services

The WY service refers to water resource production and the sequestration capacity of ecosystems in regions under the influence of natural conditions and human activities, which are affected by land-use and land cover change. In the InVEST model, the WY service comprises mainly precipitation and actual evapotranspiration, where actual evapotranspiration is obtained from the potential evapotranspiration under the constraints of soil depth and plant usable moisture content of plant roots. Therefore, the formula for calculating the WY service is as follows:

$$Y_{xi} = \left(1 - \frac{AET_{xi}}{P_x}\right) \times P_x, \quad (1)$$

where Y_{xi} is annual water yield (mm) on grid x for land-use type i, P_x is annual precipitation (mm) on grid x, and AET_{xi} is annual actual evapotranspiration (mm).

When it is a vegetation land-use type, the formula for calculating the annual actual evapotranspiration (mm) is as follows:

$$\frac{AET_{xi}}{P_x} = 1 + \frac{PET_{xi}}{P_x} - \left[1 + \left(\frac{PET_{xi}}{P_x}\right)^{w_x}\right]^{\frac{1}{w_x}}$$

The PET_{xi} is the annual potential evapotranspiration (mm) on the raster, x, when the land-use type is i, and w_x is the non-physical parameter of the soil characteristics of the natural climate.

For other land-use types, the formula for calculating annual actual evapotranspiration (mm) is as follows:

$$AET_{xi} = Min\left[K_c(\varphi_i) \times ET_{0(x)}, P_x\right]$$

where $K_c(\varphi_i)$ is the evapotranspiration coefficient of vegetation for land-use type i, and $ET_{0(x)}$ is the reference evapotranspiration of vegetation on the grid x (mm).

The potential evapotranspiration (mm) is affected by the usable water content of vegetation and the depth of the root confined layer, and is calculated as follows:

$$PET_{xi} = K_c(\varphi_i) \times ET_{0(x)}$$

$$ET_{0(x)} = 0.0013 \times 0.408 \times RA \times \left(T_{avg} + 17\right) \times \left(TD - 0.0123P\right)^{0.76}$$

Among them, RA is the radiation of the solar atmosphere (MJ/mm/d), T_{avg} is the average value of the daily maximum temperature and the daily minimum temperature

(°C), *TD* is the difference between the daily maximum temperature value and the minimum temperature value (°C), and *P* is the monthly precipitation (mm).

The formula for calculating the available water content of vegetation *PAWC* is

$$PAWC = 54.509 - 0.132 \times \text{Sand} - 0.003 \times \text{Sand}^2 - 0.055 \times \text{Silt} - 0.006 \times \text{Silt}^2 - 0.738 \times \text{Clay} + 0.007 \times \text{Clay}^2 - 2.688 \times OM + 0.501 \times OM^2$$

Among them, Sand is the soil sand content (%), Silt is the soil silt rate (%), Clay is the soil clay rate (%), and *OM* is the soil organic matter content (%).

The range of the seasonal constant, *Z*, is 1–30, the larger the value represents the regional precipitation concentrated in the second half of the year, and the smaller the value represents the precipitation concentrated in the first half of the year.

$$Z = \frac{(w_x - 1.25)P_x}{AWC_x}$$

$$AWC_x = Min(Rest.layer.depth, root.depth) \times PAWC$$

where AWC_x is the effective moisture content of the soil, *Rest.layer.depth* is the minimum root depth limiting layer, and *root.depth* is the rooting depth of vegetation.

Global Biophysical Parameters of Water Production Services is shown in Table 1.

Table 1. Global Biophysical Parameters of Water Production Services.

Lulc_Name	Lulc_Veg	Root_Depth	Kc
Agriculture	1	1000	0.672
Forest	1	5000	1.008
Grassland	1	2000	0.935
Wetland	0	−1	0.834
Settlement	0	−1	0
Shrubland	1	2500	0.800
Sparse vegetation	1	1500	0.350
Bare area	0	−1	0.200
Water	0	−1	1
Snow/Ice	0	−1	0

2.2.2. Carbon Stock Services

The CS service refers to the ability of an ecosystem to absorb and store carbon in the natural environment within the ecosystem through processes such as plant photosynthesis and organic matter production. In the InVEST model, the amount of carbon currently stored in the ecosystem is estimated through land use/land cover data and four carbon pools: aboveground biochar, belowground biochar, soil carbon, and dead organic carbon. The formula for calculating the CS service is as follows:

$$C_{total_x} = C_{above_x} + C_{below_x} + C_{soil_x} + C_{dead_x}, \quad (2)$$

where C_{total_x} is the carbon storage (*t*) on grid *x*, C_{above_x} is the aboveground carbon storage (*t*) on grid *x*, C_{below_x} is the underground carbon storage (*t*) on grid *x*, C_{soil_x} is the soil carbon storage (*t*) on grid *x*, and C_{dead_x} is the dead organic carbon storage (*t*) on grid *x*.

Global Biophysical Parameters for Carbon Stock Services is shown in Table 2.

Table 2. Global Biophysical Parameters of Carbon Stock Services.

Lulc_Name	*C_above*	*C_below*	*C_soil*	*C_dead*
Agriculture	3	2	8	1
Forest	140	70	35	12
Grassland	15	35	30	4
Wetland	1	0	0	0
Settlement	5	5	12	2
Shrubland	30	30	30	13
Sparse vegetation	20	20	20	5
Bare area	1	1	0	0
Water	0	0	0	0
Snow/Ice	0	0	0	0

2.2.3. Soil Conservation Services

The *SDR* service is an important ecosystem regulation, which is an important guarantee to prevent regional soil degradation and reduce the risk of flood disasters. In the InVEST model, the current soil conservation of the ecosystem is obtained by subtracting the actual soil erosion under artificial management and conservation measures (*ULSE*) from the potential soil erosion under natural vegetation protection (*RKLS*) according to the soil erosion equation. The formula for calculating the *SDR* service is as follows:

$$SDR_x = RKLS_x - ULSE_x, \tag{3}$$

$$RKLS_x = R_x \times K_x \times LS_x, \tag{4}$$

$$USLE_x = R_x \times K_x \times LS_x \times C_x \times P_x, \tag{5}$$

where SDR_x is the soil conservation amount (t) on grid x, $RKLS_x$ is the potential soil erosion (t) on grid x, $ULSE_x$ is the actual soil erosion (t) on grid x, R is the rainfall erosivity factor, K is the soil erodibility factor, LS is the slope length factor, C is the vegetation cover factor, and P is the soil conservation measure factor.

The formula for calculating the rainfall erosivity factor is as follows:

$$= \sum_{i=1}^{12} 1.735 \times 10^{1.5\lg \frac{P_i^2}{P} - 0.8188}$$

where P is the annual rainfall (mm) and P_i is the monthly rainfall (mm).

The formula for calculating the soil erodibility factor is as follows:

$$K = \left(-0.01383 + 0.51575 K_{epic}\right) \times 0.1317$$

$$K_{epic} = \left\{0.2 + 0.3exp\left[-0.0265 Sand\left(1 - \frac{Silt}{100}\right)\right]\right\} \times \left(\frac{Silt}{Clay + Silt}\right)^{0.3} \times \left[1 - \frac{0.25OC}{OC + exp(3.72 - 2.95OC)}\right] \times \left[1 - \frac{0.7SN}{SN + exp(22.9SN - 5.51)}\right]$$

$$SN = 1 - \frac{\text{Sand}}{100}$$

Among them, Sand is the sand content (%), Silt is the silt content (%), Clay is the clay content (%), and OC is the organic carbon content (%).

Global Biophysical Parameters for Soil Conservation Services is shown in Table 3.

Table 3. Global Biophysical Parameters for Soil Conservation Services.

Lulc_Name	Usle_c	Usle_p
Agriculture	0.30	1
Forest	0.03	1
Grassland	0.08	1
Wetland	1	1
Settlement	0	0
Shrubland	0.06	1
Sparse vegetation	0.01	1
Bare area	1	1
Water	0	0
Snow/Ice	0	0

2.2.4. Habitat Quality Services

Biodiversity is closely linked to ESS production. The HQ module in the InVEST model can estimate the HQ in the current ecosystem by analyzing land use/land cover and threats to species habitats. In this study, farmland, unused land, and construction land were selected as threat sources, in accordance with the InVEST manual and other relevant literature, parameters, such as the maximum impact distance and weight of threat sources, as well as the sensitivity of land-use types to threat sources were derived [34,35]. The formula for calculating the HQ service is as follows:

$$D_{xi} = \sum_{r=1}^{R} \sum_{y=1}^{Y_r} \left(\frac{W_r}{\sum_{r=1}^{R} W_r} \right) r_y i_{rxy} \beta_x S_{ir}, \quad (6)$$

$$Q_{xi} = H_i \left(1 - \left(\frac{D_{xi}^z}{D_{xi}^z + K^z} \right) \right), \quad (7)$$

where Q_{xi} is the HQ score of raster x for land-use type i, D_{xi} is the habitat degradation degree of raster x, R is the number of threat factors, y is the number of rasters on the threat raster map, Y_r is the number of rasters on the raster map of the threat factor r, Y_r is the weight of the threat factor, r_y is the threat intensity, i_{rxy} is the threat level, β_x is the degree of legal protection (the greater the degree, the smaller the threat), S_{ir} is the sensitivity of land-use type, i, to threat factor, R (the closer the value of R is to 1, the stronger the sensitivity), H_i is the habitat suitability, K is the semi-saturated parameter (initially set to 0.5, then subsequently set to half the maximum habitat degradation), and Z is the normalization constant.

2.2.5. Grading Basis

To better understand the spatiotemporal variations in waterfront ESS globally, this study classified four ecosystem services (i.e., WY, CS, SDR, and HQ) and the total supply of waterfront ESS globally using the natural breakpoint method, and the characteristics of their spatiotemporal variation during 2010–2020 were analyzed. In this study, ESS were divided into seven levels, with level 1 (7) representing the worst (best) ESS in the region.

2.2.6. Trade-Off Synergy Analysis

Based on the raster data of the four ESS during 2010–2020, this study used the "Create Fishing Net" tool in ArcGIS software to generate 10,000 sampling points in waterfront areas globally and extracted the corresponding ESS values of each point. Then, Spearman's coefficient was used to test the trade-off synergies between the four ecosystem services. A value of $r > 0$ indicates a synergistic relationship; a value of $r < 0$ indicates a trade-off relationship, and a value of $r = 0$ indicates no correlation. The magnitude of the value

reflects the strength of the relationship between ESS pairs. Finally, based on the R Studio platform, both the trade-offs and the synergies between waterfront ESS globally were visualized and the results analyzed.

2.3. Data Sources

The data used in this study for assessment of waterfront ESS globally are listed in Tables 4 and 5.

Table 4. Value of ecosystem services by province in 2020.

Province	WY (mm)	CS ($\times 10^8$ t)	SDR ($\times 10^8$ t)	HQ
National	400.24	25.67	132.17	0.68
Anhui	864.16	0.81	0.72	0.54
Beijing	134.18	0.04	0.06	0.63
Chongqing	816.14	0.54	1.81	0.52
Fujian	827.26	0.17	0.79	0.68
Gansu	146.48	0.44	0.83	0.76
Guangdong	1085.53	0.84	1.69	0.43
Guangxi	711.12	1.2	3.63	0.74
Guizhou	657.41	0.45	1.88	0.8
Hainan	772.35	0.01	0.03	0.98
Hebei	146.63	0.41	0.23	0.48
Henan	388.62	0.71	0.2	0.36
Heilongjiang	222.8	1.89	0.67	0.65
Hubei	911.56	1.49	3.71	0.52
Hunan	933.32	1.34	1.97	0.54
Jilin	218.06	0.66	0.75	0.63
Jiangsu	794.97	0.85	0.11	0.49
Jiangxi	1100.7	1.03	0.69	0.6
Liaoning	293.91	0.33	0.39	0.49
Inner Mongolia	65.93	1.63	0.32	0.72
Ningxia	2.87	0.27	0.01	0.49
Qinghai	149.3	1.15	4.42	0.93
Shandong	288.88	0.57	0.07	0.34
Shanxi	162.25	0.48	0.32	0.53
Shaanxi	260.3	0.57	1.54	0.64
Shanghai	841.71	0.26	0.01	0.37
Sichuan	415.84	1.71	23.51	0.75
Taiwan	2182.24	0.05	1.67	0.52
Tianjin	218.5	0.03	0.01	0.2
Tibet	175.65	2.11	43.66	0.97
Xinjiang	2.16	0.56	0.12	0.56
Yunnan	411.51	2.78	47.61	0.86
Zhejiang	1011.01	0.25	0.98	0.64

Table 5. Ecosystem services assessment dataset.

The Name of the Data	Data Source	Data Download Link
DEM dataset	Zhang et al., 2022 [36]	https://doi.org/10.1016/j.scib.2022.11.021, accessed on 5 February 2024.
Land cover classification	Store, 2019 [37]	http://doi.org/10.24381/cds.006f2c9a, accessed on 10 February 2024.

Table 5. *Cont.*

The Name of the Data	Data Source	Data Download Link
Monthly high-resolution gridded multivariate climate dataset	Harris et al., 2020 [38]	https://doi.org/10.1038/s41597-020-0453-3, accessed on 5 February 2024.
ETMonitor Global Actual Evapotranspiration Dataset	Zheng, 2022 [39]	https://doi.org/10.1016/j.jhydrol.2022.128444, accessed on 15 March 2024.
Harmonized World Soil Database v 1.2	Fischer et al., 2008 [40]	https://www.fao.org/soils-portal/soil-survey/soil-maps-and-databases/harmonized-world-soil-database-v12/en/, accessed on 20 March 2024.

3. Results

3.1. Changes in Spatiotemporal Patterns of Waterfront Ecosystem Services Globally

The spatiotemporal variations in WY, CS, SDR, and HQ in waterfronts globally during 2010–2020 are shown in Figure 2. Overall, WY showed a trend of increase, initially decreasing from an annual average of 124.67 mm in 2010 to an annual average of 111.45 mm in 2015, but then increasing to an annual average of 127.92 mm in 2020. Spatially, WY was generally high in the south and low in the north, and the high-value areas were mainly in the northwest of the United Kingdom and the southwest of Norway in Europe, the southeast of China in Asia, the south of Myanmar, the west and east of Indonesia, and the northern part of Guyana and northwestern part of Brazil in South America. During 2010–2020, there was substantial increase in WY in southwestern Norway in Europe, the southeastern United States in North America, and northern Brazil in South America, whereas Portugal in Europe, western Iraq, southeastern China, eastern Indonesia in Asia, western Papua New Guinea, and Venezuela in South America showed a downward trend.

The trend in CS was downward during 2010–2020, from 128.8 billion tons in 2010 to 127.8 billion tons in 2020. Spatially, the high-value areas of CS were mainly in Norway, Sweden, and Finland in Europe, the Democratic Republic of the Congo in Africa, Russia, southern China, North Korea, and South Korea in Asia, Canada in North America, and Guyana, Peru, and northwestern Brazil in South America, whereas the low-value areas were mainly in the areas around lakes and rivers.

Contrary to CS, SDR increased from 2.575 billion tons in 2010 to 2.690 billion tons in 2020. Spatially, SDR was poor overall, although it was highest in southwest China in Asia and central Peru in South America.

The distribution of HQ was the opposite to that of SDR, and it was generally higher overall. The low-value areas were mainly in Algeria, Libya, and Niger in Africa and in Saudi Arabia, Oman, Yemen, and Iraq in Asia.

In summary, the results of the changes in waterfront ESS globally during 2010–2020 are shown in Figure 3. The ESS of waterfront areas in all continents showed a spatial pattern of being high in the north and low in the south, except for Africa, which showed a pattern of being high in the south and low in the north. The high-value areas were mainly in Sweden and Finland in Europe, the Democratic Republic of the Congo in Africa, Russia, Southwestern China, and Indonesia in Asia, the Northwestern United States and Canada in North America, and northeastern Peru and northwestern Brazil in South America. During 2010–2020, there was little change in ESS overall, but notable decline occurred in northwestern parts of the Democratic Republic of the Congo in Africa and northwestern parts of Brazil in South America.

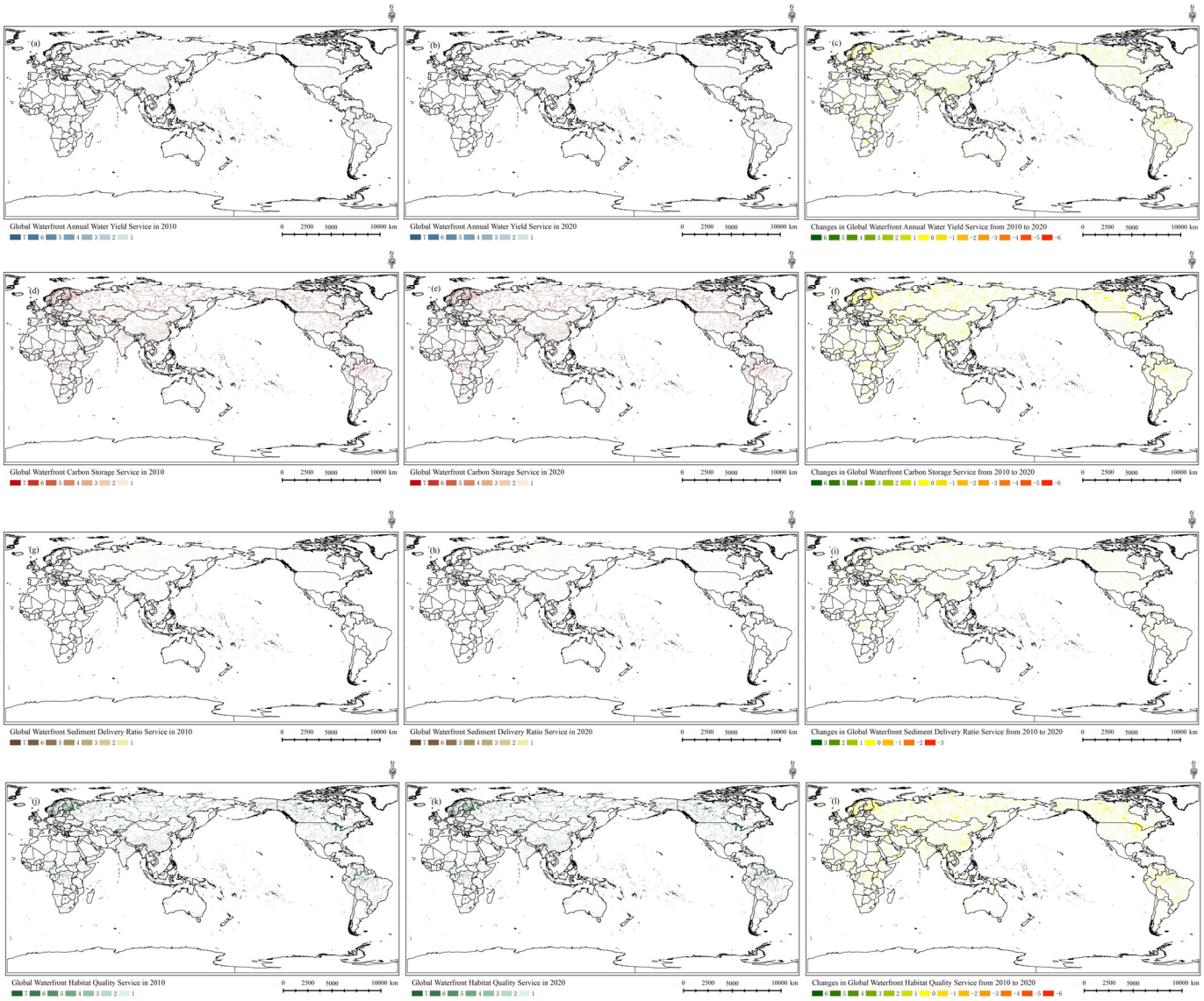

Figure 2. Spatiotemporal distributions of four ecosystem services in waterfronts globally during 2010–2020. (**a**–**c**) shows WY in 2010, 2020, and from 2010 to 2020; (**d**–**f**) shows CS in 2010, 2020, and from 2010 to 2020; (**g**–**i**) shows SDR in 2010, 2020, and from 2010 to 2020; (**j**–**l**) shows WY in 2010, 2020, and from 2010 to 2020.

From the perspective of the spatiotemporal variations in ESS in each continent, South America had the highest WY and SDR, Asia had the highest CS, and North America had the highest average HQ score, as shown in Figure 4. During 2010–2020, WY in Asia, Africa, and South America showed an initial downward trend followed by an increase, whereas WY in Europe, North America, and Oceania showed a trend of initial increase followed by decline. Except for South America and Oceania, WY in all other continents showed a trend of increase relative to that in 2010. Except for Africa, CS showed a downward trend during 2010–2020 in all continents, in accordance with the overall global trend; CS in Africa increased from 11.4 billion tons in 2010 to 11.5 billion tons in 2020. During 2010–2020, the trend of change in SDR was markedly different in various continents. In Asia, SDR increased from 294 million tons in 2010 to 321 million tons in 2020. Generally, SDR in Europe and Africa first declined and then increased, rising by 5 million and 60 million tons, respectively, compared with that in 2010. In North America, South America, and Oceania, SDR ultimately decreased 266 million, 452 million, and 23 million tons, respectively, in 2010 to 258 million, 343 million, and 20 million tons, respectively, in 2020. Overall, HQ changed

little during 2010–2020, with North America having the highest average HQ score of 0.91 and Africa having the lowest average score of 0.64.

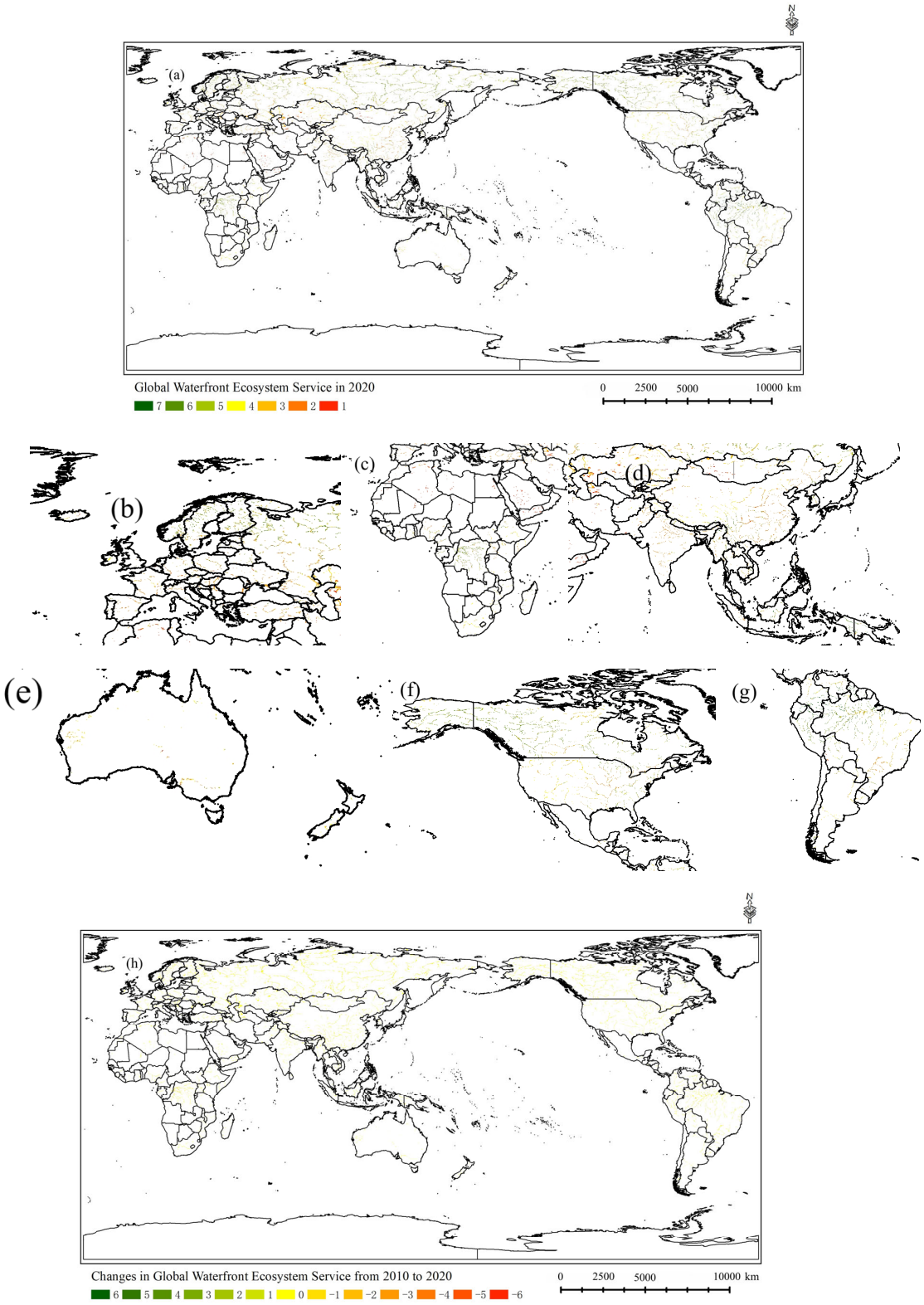

Figure 3. (**a**) Spatiotemporal changes in ecosystem services in waterfronts globally in 2020. Detailed: (**b**): Europe; (**c**): Africa; (**d**): Asia; (**e**): Oceania; (**f**): North America; (**g**): North America; (**g**): Changes in Global Waterfront Ecosystem Service from 2010 to 2020; (**h**): Spatiotemporal changes in ecosystem services in waterfronts globally during from 2010 to 2020.

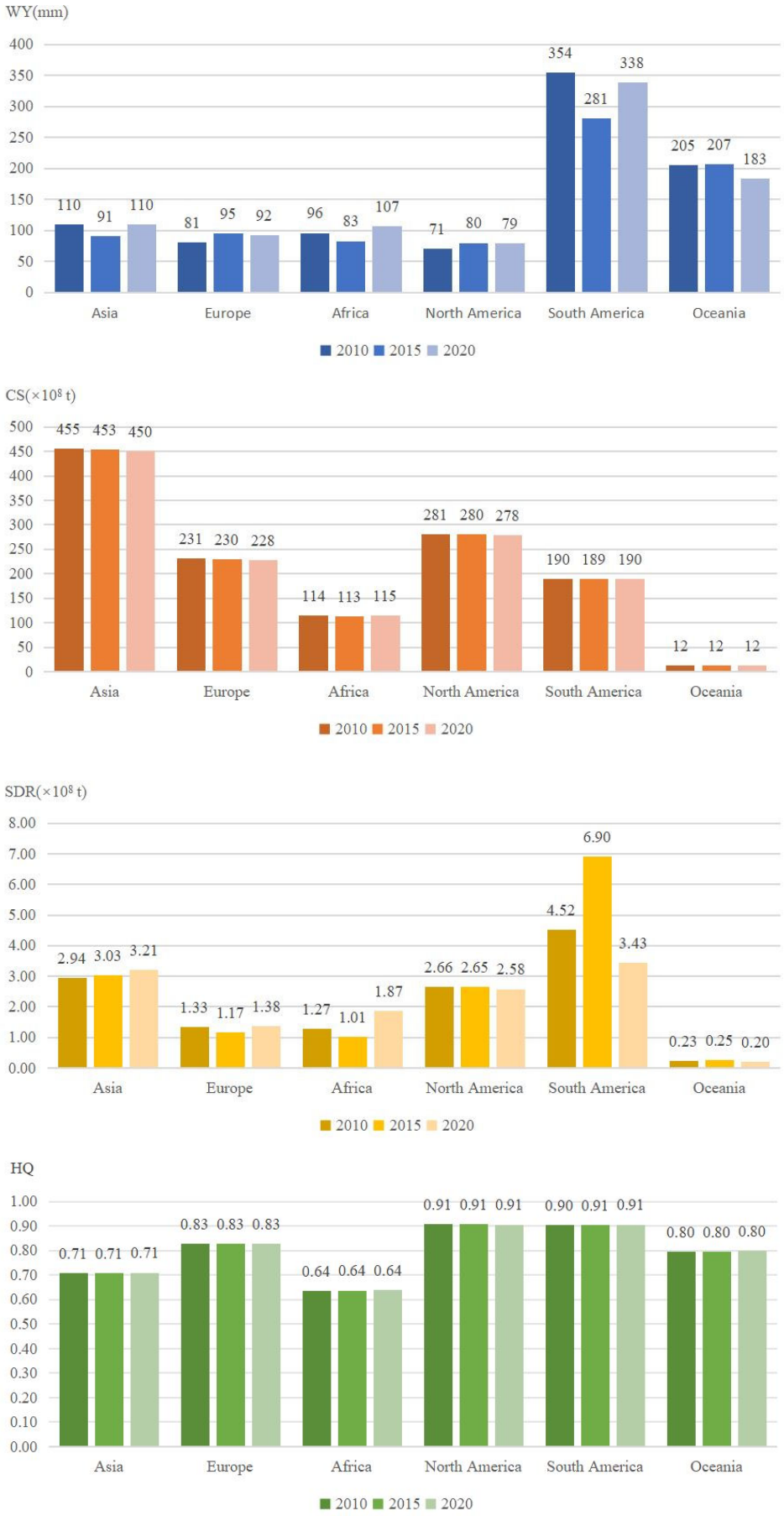

Figure 4. Changes in ecosystem services in waterfront areas globally during 2010–2020.

3.2. Synergistic Analysis of Ecosystem Service Trade-Offs in Waterfronts Globally

The Spearman correlation coefficients between WY, CS, SDR, and HQ in 2010, 2015, and 2020 are shown in Figure 5. There are six pairs of trade-offs and synergistic correlations among the four ESS that changed over time. During 2010–2020, there was prominent negative correlation between WY and HQ, indicating an obvious trade-off relationship, and the trade-off effect increased during 2010–2015 and weakened during 2015–2020. However, the trade-off effect showed a characteristic of overall enhancement during 2010–2020. The correlation coefficient between WY and CS was positive, indicating a synergistic relationship, and the synergy showed a gradual trend of increase during 2010–2020. The synergistic effect between WY and SDR was similar to that between WY and HQ, and it also exhibited the characteristics of initial strengthening and then weakening. There was a diminishing synergistic relationship between CS and SDR and between CS and HQ. The correlation between SDR and HQ was not significant, with a value of 0.00 in both 2010 and 2015, but there was a trade-off in 2020.

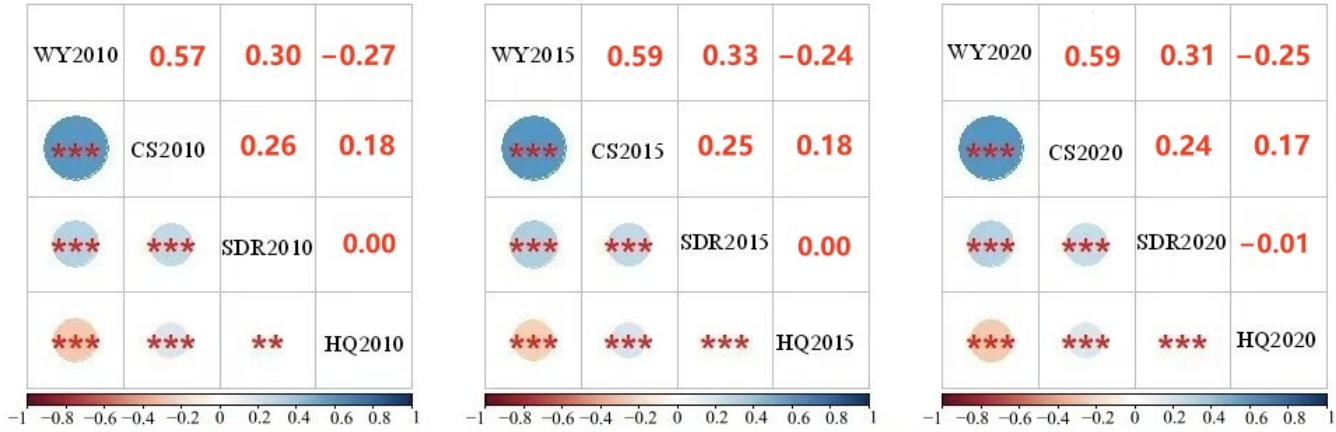

Figure 5. Trade-offs and synergies of ecosystem services in waterfront areas globally. Notes: *** and ** indicate statistical significance at the 1%,5% levels, respectively.

Specifically, in 2020, there was a strong trade-off between WY and HQ in Asia and North America, and the trade-off was greater than the global average. The synergy between WY and CS in South America was notably stronger than the global average at 0.76. The synergy between WY and SDR was higher than the global average in Europe but lower than the global average in North America. Moreover, the synergy between CS and HQ was very significant in the waterfront areas of all continents, with the strongest (weakest) synergy in Africa (Europe) at 0.49 (0.13).

3.3. Spatiotemporal Pattern of Ecosystem Services in China's Waterfronts

To further analyze the relationship between waterfront ESS and land-use change and to provide suggestions for sustainable development of waterfronts, this study investigated the spatiotemporal changes, trade-offs, and synergies of waterfront ESS in China during 2000–2020.

3.3.1. Spatiotemporal Changes in Land Use in China's Waterfronts

The land-use types of China's waterfronts are mainly farmland (28.71%) and water area (27.93%), and they are distributed mainly on the North China Plain and in the middle–lower reaches of the Yangtze River. The provinces in which the cities or famous attractions mentioned above are located are shown in Table 6. The water areas of the Qinghai–Tibet Plateau are more widely distributed, e.g., Mapanyongcuo, Yangzhuo Yongcuo, Namco, and Qinghai Lake. Grassland (18.11%) is distributed mainly on the Qinghai–Tibet Plateau,

and forest (14.16%) is distributed mainly in Southwestern China, e.g., Nyingchi in Tibet, Yunnan, Baise, and Hechi in Guangxi, and the Ganzi Tibetan Autonomous Prefecture, Aba Tibetan and Qiang Autonomous Prefecture, and Liangshan Yi Autonomous Prefecture in Sichuan. Land-use types such as construction land (6.58%) and unused land (3.97%) are distributed in a small area.

Table 6. Cities or Lakes of provinces in China.

Province	Cities or Famous Attractions
Tibet	Nyingchi, Mapanyongcuo, Yangzhuo Yongcuo, Namco
Qinghai	Qinghai Lake
Yunnan	Baise, Nujiang Lisu Autonomous Prefecture, western Dali Bai Autonomous Prefecture, Lincang, Pu'er
Guangxi	Hechi, Ganzi Tibetan Autonomous Prefecture, Aba Tibetan and Qiang Autonomous Prefecture, Laibin, Guigang
Sichuan	Liangshan Yi Autonomous Prefecture
Hunan	Yiyang, Yueyang, Jiujiang, Chenzhou
Guangdong	Foshan, Zhongshan, Dongguan

During 2000–2020, except for forest and water area, land use types showed a trend of increase in area compared with the values in 2000, especially grassland and farmland, which increased by 0.17% and 0.14%, respectively; conversely, forest and water area decreased by 0.47% and 0.02%, respectively. Figure 6 shows that the area of grassland increased substantially, mainly because of the conversion of 16.22% of the ice and snow area, 14.93% of the unused land area, and 11.40% of the shrub area. Additionally, 10.06% of forest, 9.57% of water, and 8.19% of shrub areas were converted into farmland, resulting in the second largest increase in farmland area. In addition to the conversion of some forest to farmland, 6.39% of forest was converted to grassland, resulting in a total of only 14.16% of the waterfront areas.

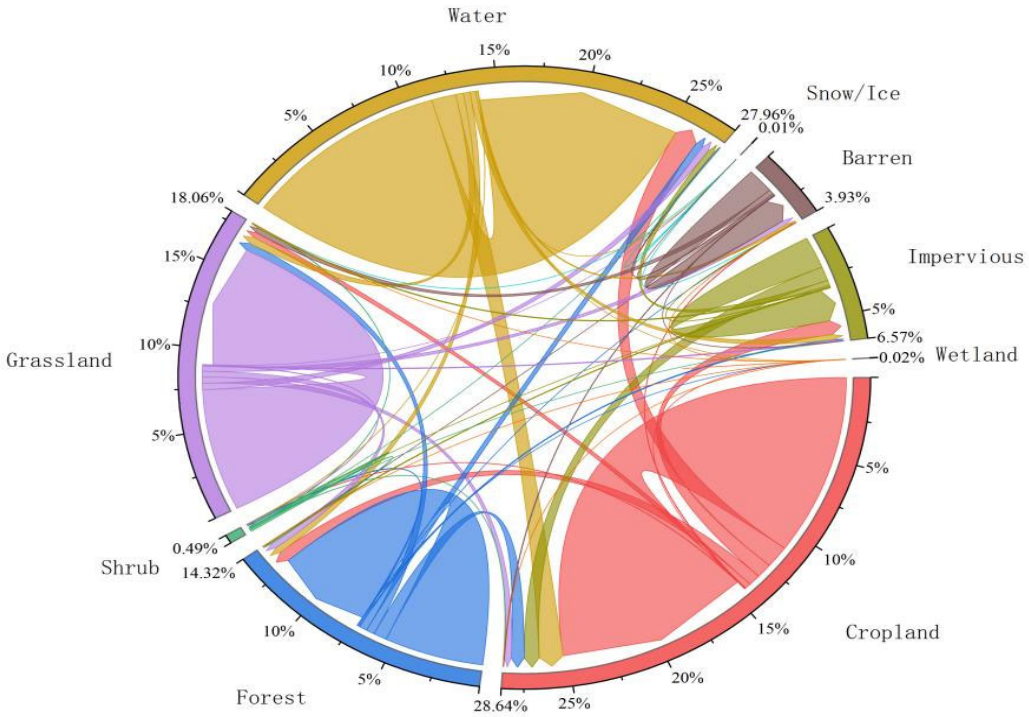

Figure 6. Area transfer map of waterfront land-use types in China during 2000–2020.

3.3.2. Spatiotemporal Variation in Ecosystem Services in China's Waterfronts

The spatial distributions of WY, CS, SDR, HQ, and total ESS supply in China's waterfronts during 2000–2020 are shown in Figure 7. The results show that the ESS in waterfront

areas in China generally showed a spatial pattern of low (high) in the north (southwest). Overall, ESS were higher in Nyingchi in Tibet, Nujiang Lisu Autonomous Prefecture in Yunnan, western Dali Bai Autonomous Prefecture, Lincang, and Pu'er in Yunnan, Hechi, Laibin, and Guigang in Guangxi, Yiyang and Yueyang in Hunan, and Jiujiang, Nanchang, and Shangrao in Jiangxi.

Specifically, during 2000–2020, WY in China's waterfront areas showed an upward trend, increasing from an annual average of 355.49 mm to an annual average of 400.24 mm, and the high-value areas were distributed mainly in the southwest of Nyingchi City in Tibet, the northeast of Jiangmen City in Guangdong, and northern and southwestern parts of Taiwan. During 2000–2020, CS decreased from 2.668 billion to 2.567 billion tons, and the decline was distributed mainly in Foshan City, the northeast of Zhongshan City, the southwest of Guangzhou City, and the northwest of Dongguan City. Similarly, SDR also showed a downward trend, decreasing from 15.011 billion to 13.217 billion tons, and the distribution of its high-value areas was similar to that of water production, i.e., mainly in the southern part of Nyingchi City in Tibet and the southwestern part of Taiwan. Overall, HQ showed a trend of increase during 2000–2020, similar to WY, but the distribution of its high-value areas was the opposite to that of WY, i.e., occurring mainly in surrounding areas of lakes and rivers such as Chenzhou City in Hunan, Hangzhou City in Zhejiang, and Miyun District in Beijing. Table 7 lists the values of ESS in each province of China in 2020.

Table 7. Relevance of ecosystem services in China's waterfronts from 2000 to 2020.

ES	WY			CS			SDR			HQ		
	2010	2015	2020	2010	2015	2020	2010	2015	2020	2010	2015	2020
WY	1	1	1	0.46 ***	0.45 ***	0.35 ***	0.27 ***	0.26 ***	0.23 ***	−0.13 ***	−0.21 ***	−0.32 ***
CS	0.46 ***	0.45 ***	0.35 ***	1	1	1	0.21 ***	0.21 ***	0.21 ***	0.03 ***	0.09 ***	0.11 ***
SDR	0.27 ***	0.26 ***	0.23 ***	0.21 ***	0.21 ***	0.21 ***	1	1	1	0.22 ***	0.21 ***	0.19 ***
HQ	−0.13 ***	−0.21 ***	−0.32 ***	0.03 ***	0.09 ***	0.11 ***	0.22 ***	0.21 ***	0.19 ***	1	1	1

Notes: *** indicates statistical significance at the 1% level.

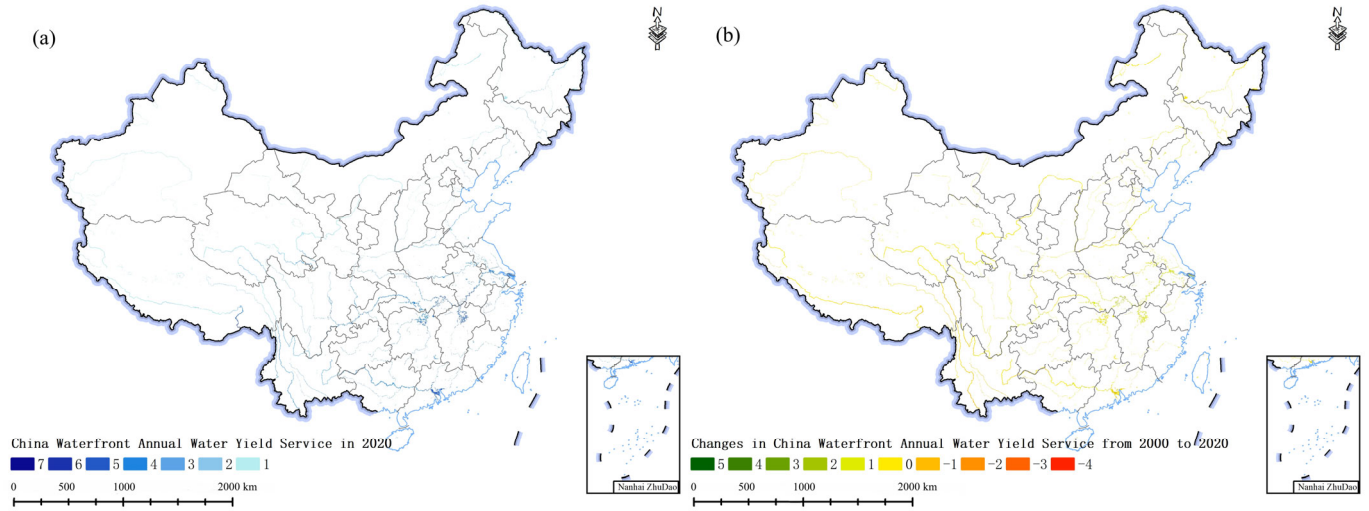

Figure 7. *Cont.*

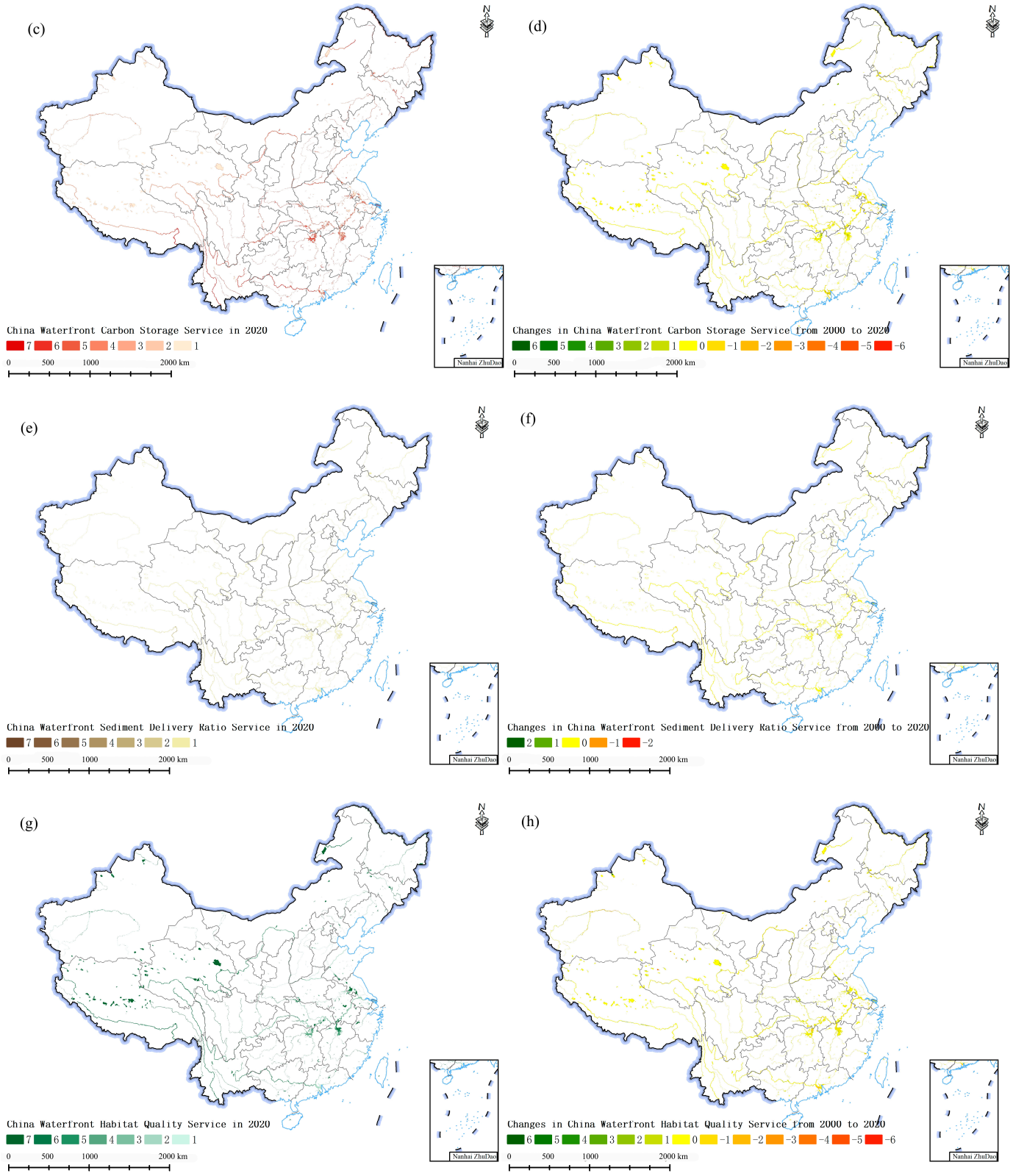

Figure 7. *Cont.*

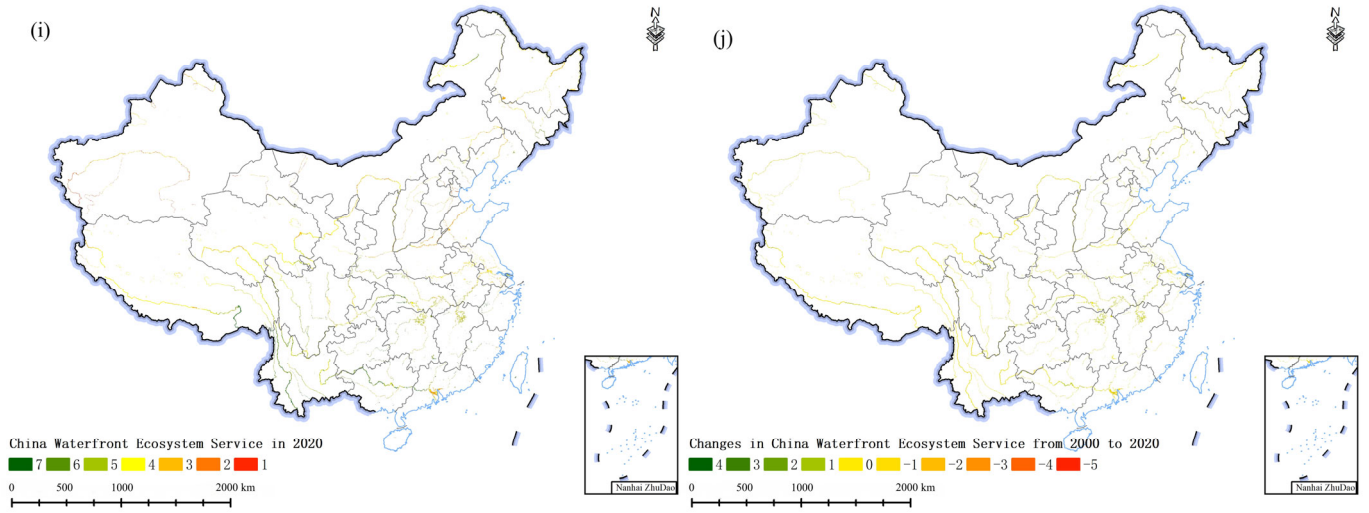

Figure 7. Spatiotemporal variation in ecosystem services in China's waterfronts during 2000–2020. (**a**,**b**): WY2010, 2000–2020; (**c**,**d**): CS2010, 2000–2020; (**e**,**f**): SDR2010, 2000–2020; (**g**,**h**): SDR2010, 2000–2020; (**i**,**j**): ES2010, 2000–2020.

3.4. Synergistic Analysis of Ecosystem Service Trade-Offs in China's Waterfronts

Table 7 presents Spearman's correlation coefficients between WY, CS, SDR, and HQ in China's waterfronts during 2000–2020. Except for the trade-off between WY and HQ, there were notable synergies between the other services. Among them, the synergy between WY and CS (CS and HQ) was the strongest (weakest). During 2000–2020, except for the marked increase in synergy between CS and HQ (i.e., from 0.03 to 0.11), the synergies between WY and CS, WY and SDR, and SDR and HQ all showed a weakening trend, and the synergy between WY and CS decreased the most.

4. Discussion

4.1. Analysis of the Influencing Factors

Influencing Factors of Ecosystem Services in Waterfront Areas

Based on comprehensive analysis of the spatiotemporal variation characteristics of four ecosystem services in waterfronts globally and in China during 2010–2020, this study found that WY showed a fluctuating upward trend, which might be attributable to increase in both construction land area and unused land area. During 2010–2020, the area of construction land in waterfront areas increased by 26.06%, showing a rapid trend of growth. Most construction land is characterized by hardened pavement such as cement, and, therefore, the amount of precipitation infiltration is reduced, resulting in higher WY [8,41]. Additionally, areas with high vegetation coverage, such as forest and shrub, account for more than 30% of the area of waterfronts globally and, therefore, the transpiration of vegetation and the water storage capacity of the soil will lead to lower WY, accounting for a small increase in WY [33].

Overall, CS declined in waterfronts globally and in China, which might reflect the impact of rapid socioeconomic development, which has expanded the area of construction land and occupied ecological land, resulting in decline in carbon sequestration capacity [42]. Additionally, areas with high values of CS are distributed mainly in areas with high vegetation coverage, such as forest, and the areas of forest and shrub in waterfronts globally and in China are declining, resulting in the downward trend in CS [10,43].

In most waterfront areas globally and in China, SDR performed poorly because the waterfront land type is dominated by water, and there is almost no land evolution in waterfront areas, resulting in weak soil conservation capacity in waterfront areas [44].

During 2010–2020, the SDR of waterfronts globally showed a trend of increase, mainly because the area of forest accounted for a relatively large area, the area of construction land increased, and the area of unused land decreased, which reduced soil erosion and enhanced the soil and water conservation capacity. During 2000–2020, the SDR in waterfront areas in China showed a notable downward trend compared with that of waterfronts globally, mainly because the area of forest decreased substantially, and the area of shrub changed little.

The distribution of high-value HQ areas was similar to that of CS, owing to the high vegetation coverage and low intensity of human activities in areas such as forest, grassland, and wetlands [45].

4.2. Trade-Offs and Synergistic Changes in Waterfront Ecosystem Services

There is a strong synergistic relationship between WY, CS, and SDR, which reflects the fact that areas with higher WY have better tree growth and higher vegetation cover, thereby promoting carbon storage and attenuating soil erosion [42,44]. The observed weakening of the synergies between WY and CS and between WY and SDR in waterfront areas in China reflects the reduction in forest area and the increase in both construction land area and unused land area, which promotes increased WY but reduced CS [8]. Moreover, areas with high vegetation coverage, such as forest and shrub, have strong capacity to intercept rainfall and play a positive role in resisting soil erosion, which has negative impact on WY [8,42]. The synergy between CS and SDR in waterfronts globally and in China is gradually weakening because grassland and farmland account for a high proportion of waterfront areas, and they show a trend of increase. However, vegetation in grassland and farmland has low root depth and the soils are prone to erosion via landslides and debris flows, resulting in weak SDR [14]. Conversely, plant photosynthesis and carbon sequestration by the roots of vegetation in farmland and grassland areas have positive impact on CS, thereby weakening the synergistic effect [10,46].

There is also a strong synergy between CS, SDR, and HQ. The strong synergy between CS and HQ in waterfront areas is attributable to the increase in CS related to vegetation, such as forest and shrub, as well as the lower intensity of human activities in areas with higher vegetation coverage, and both promote HQ development [45]. Moreover, in areas with high HQ, high vegetation coverage and weak soil erosion enhance SDR; consequently, such areas have strong synergy between SDR and HQ [14,44]. The synergy between CS and HQ in waterfronts globally gradually weakened during 2010–2020, owing to the trend of decline in forest and shrub areas, and the trend of increase in grassland area; however, the grassland was more disturbed by human activities, resulting in poor HQ and weakened synergy [45]. The main reason for the gradual increase in the trade-off relationship between SDR and HQ is that increase in construction land area leads to deterioration in HQ, while SDR increases; thus, the relationship between the two changes from a very low synergistic relationship to a trade-off relationship.

4.3. Recommendations

In the process of urbanization, construction land should be rationally planned to avoid excessive expansion and occupation of ecological land, especially woodland, shrubs and other areas with high ecological value.

In view of the weak SDR (soil conservation capacity) in waterfront areas [47], vegetation restoration and protection should be strengthened, especially the protection and restoration of forest land, to improve soil conservation capacity.

In areas that are prone to soil erosion, soil and water conservation projects, such as the construction of terraces, grass planting, slope protection, etc., are implemented to reduce

soil erosion. Meanwhile, the government should introduce policies to encourage and support ecological protection and restoration, such as providing financial subsidies and tax incentives [48,49].

In summary, the sustainable development of ecosystem services in waterfront areas can be promoted and the harmonious coexistence of urbanization and ecological protection can be realized through rational planning of construction land [50], improvement of soil and water conservation capacity, enhancement of carbon storage and sequestration capacity, improvement of habitat quality, strengthening of collaborative management of ecosystem service trade-offs, and policy guidance and public participation.

5. Conclusions

Based on the physical geographical characteristics and ecological environments of waterfronts, the four key ESS of WY, CS, SDR, and HQ were selected in this study to evaluate both the spatiotemporal changes and the trade-offs and synergies of ESS globally and in China [24,42]. The results showed that WY, SDR, and HQ in waterfronts globally increased during 2010–2020, whereas CS showed a trend of decline. The areas with greatest increases in ESS were mainly the northwest of the Democratic Republic of the Congo, Southwestern China, and northeastern Peru. Except for the trade-off between WY and HQ, the ESS of waterfronts globally exhibited strong synergy. The trend of ESS in China's waterfronts was broadly the same as that of waterfronts globally, with a downward trend except for SDR. Additionally, China's waterfronts showed notable growth in Laibin and Guigang in Guangxi, Yiyang, Yueyang, and Changde in Hunan, Nanchang, Jiujiang, and Shangrao in Jiangxi, Jingzhou, Yichang, Wuhan, and Ezhou in Hubei, and Anqing, Tongling, Wuhu, and Bengbu in Anhui [41].

6. Outlook

The results of collaborative estimation of ESS and trade-offs from the perspective of waterfront areas globally and in China, conducted in this study, provide support for sustainable development of waterfronts globally and high-quality construction of waterfront areas in China [51,52]. However, in addition to land-use change, other factors such as the climate and the economy affect ESS. Therefore, a more comprehensive approach will be considered in future work to quantitatively assess the influencing factors of waterfront ESS, identify important driving forces for improving waterfront public space and achieving sustainable development goals [53]. Additionally, regarding missing values and the accuracy of the data used (e.g., soil and evapotranspiration data), future work will select more accurate data, or missing values will be processed more effectively before analysis to prepare for smaller-scale waterfront case studies.

Author Contributions: Y.Z. (Yaomin Zheng) contributed to the conception and design of the study, performed experiments, and analyzed the data. H.Y. assisted with the experimental design and data interpretation. H.G. provided critical feedback on the manuscript and contributed to the discussion section. J.S. helped with the literature review and contributed to the writing of the introduction. J.W. was responsible for data collection and management. Y.Z. (Yanhui Zhang) assisted with statistical analysis and data visualization. X.Z. contributed to the revision of the manuscript and improved the clarity of the writing. R.C. supervised the project and provided overall guidance. Y.C. assisted with the preparation of the figures and tables. All authors have read and agreed to the published version of the manuscript.

Funding: This research was supported by the National Natural Science Foundation of China (No: 72374017), the National Social Science Fund of China (21AGL012), the Project of Cultivation for young top-notch Talents of Beijing Municipal Institutions (No: BPHR202203055), and the Key Program of the Beijing Municipal Commission of Education (No: SZ202110011006).

Informed Consent Statement: Not applicable.

Data Availability Statement: The data used in this study for assessment of waterfront ESS globally are listed in Table 3.

Acknowledgments: We thank James Buxton for editing the English text of a draft of this manuscript. We thank Qiuyun Zhao, from Institute of New Structural Economics, Peking University, for helping us on the revision.

Conflicts of Interest: The authors declare no competing interests. Regarding pending patents/patent applications, there are no relevant disclosures to report at this time. If any patents or patent applications arise in the future that are related to the work presented in this manuscript, the authors will disclose the following information: patent applicant (whether author or institution), name of the inventor(s), application number, the status of the application, and the specific aspect of the manuscript covered in the patent application.

References

1. Raymond, C.M.; Singh, G.G.; Benessaiah, K.; Bernhardt, J.R.; Levine, J.; Nelson, H.; Turner, N.J.; Norton, B.; Tam, J.; Chan, K.M.A. Ecosystem services and beyond: Using multiple metaphors to understand human–environment relationships. *BioScience* **2013**, *63*, 536–546. [CrossRef]
2. Costanza, R.; De Groot, R.; Braat, L.; Kubiszewski, I.; Fioramonti, L.; Sutton, P.; Farber, S.; Grasso, M. Twenty years of ecosystem services: How far have we come and how far do we still need to go? *Ecosyst. Serv.* **2017**, *28*, 1–16. [CrossRef]
3. Millennium Ecosystem Assessment (MEA). *Ecosystems and Human Well-Being*; Island Press: Washington, DC, USA, 2005.
4. United Nations. *Transforming Our World: The 2030 Agenda for Sustainable Development*; United Nations: New York, NY, USA, 2015.
5. Bennett, E.M.; Peterson, G.D.; Gordon, L.J. Understanding relationships among multiple ecosystem services. *Ecol. Lett.* **2009**, *12*, 1394–1404. [CrossRef] [PubMed]
6. Liu, H.-Y.; Xiao, W.-F.; Li, Q.; Tian, Y.; Zhang, Q.-R.; Zhu, J.-H. Spatiotemporal variations and trade-offs of ecosystem services in Beijing. *Chin. J. Ecol.* **2021**, *40*, 209–219. (In Chinese)
7. Wu, Y.; Zhang, X.; Li, C.; Xu, Y.; Hao, F.; Yin, G. Ecosystem service trade-offs and synergies under influence of climate and land cover change in an afforested semiarid basin, China. *Ecol. Eng.* **2021**, *159*, 106083. [CrossRef]
8. Wang, L.; Yu, E.; Li, S.; Fu, X.; Wu, G. Analysis of Ecosystem Service Trade-Offs and Synergies in Ulansuhai Basin. *Sustainability* **2021**, *13*, 9839. [CrossRef]
9. Ren, J.; Zhao, X.Y.; Xu, X.C.; Ma, P.Y.; Du, Y.X. Spatial-temporal evolution, tradeoffs and synergies of ecosystem services in the middle Yellow River. *J. Earth Environ.* **2022**, *13*, 477–490. (In Chinese)
10. Li, Z.; Cheng, X.; Han, H. Analyzing land-use change scenarios for ecosystem services and their trade-offs in the ecological conservation area in Beijing, China. *Int. J. Environ. Res. Public Health* **2020**, *17*, 8632. [CrossRef]
11. Hasan, S.S.; Zhen, L.; Miah, M.G.; Ahamed, T.; Samie, A. Impact of land use change on ecosystem services: A review. *Environ. Dev.* **2020**, *34*, 100527. [CrossRef]
12. Arunyawat, S.; Shrestha, R.P. Assessing land use change and its impact on ecosystem services in Northern Thailand. *Sustainability* **2016**, *8*, 768. [CrossRef]
13. Zhong, S.Z.; Sun, H.Y. Assessment on spatiotemporal variation and synergies/tradeoffs relationships of ecosystem services in Qilian mountain national nature reserve under different scenarios. *Res. Soil Water Conserv.* **2023**, *30*, 358–369. (In Chinese)
14. Yang, Y.; Dou, Y.; Wang, Y.; An, S. Ecosystem service tradeoffs and synergies in typical small watersheds of the hilly and gully region of the Loess Platea. *Acta Ecol. Sin.* **2022**, *42*, 8152–8168. (In Chinese)
15. Zhou, Y.G.; Shen, X.W. Research on the development orientations of urban waterfront based on space-time dimension. *Urban Probl.* **2011**, *2*, 30–35. (In Chinese)
16. Bonoli, A.; Di Fusco, E.; Zanni, S.; Lauriola, I.; Ciriello, V.; Di Federico, V. Green Smart Technology for Water (GST4Water): Life cycle analysis of urban water consumption. *Water* **2019**, *11*, 389. [CrossRef]
17. Ciampa, F.; De Medici, S.; Viola, S.; Pinto, M.R. Regeneration criteria for adaptive reuse of the waterfront ecosystem: Learning from the US case study to improve european approach. *Sustainability* **2021**, *13*, 4156. [CrossRef]
18. Avni, N.; Fischler, R. Social and environmental justice in waterfront redevelopment: The Anacostia river, Washington, DC. *Urban Aff. Rev.* **2020**, *56*, 1779–1810. [CrossRef]
19. Ferah, B.; Gemci, A.G.; Algburi, O. An analysis of the spatial qualities of the waterfronts: Conceptual proposal projects for Istanbul Sarayburnu. *Open House Int.* **2023**, *48*, 402–424. [CrossRef]
20. Üzümcüoğlu, D.; Polay, M. Urban waterfront development, through the lens of the Kyrenia waterfront case study. *Sustainability* **2022**, *14*, 9469. [CrossRef]

21. Follmann, A. Urban mega-projects for a 'world-class' riverfront–The interplay of informality, flexibility and exceptionality along the Yamuna in Delhi, India. *Habitat Int.* **2015**, *45*, 213–222. [CrossRef]
22. Zhang, H.Z.; Shen, X.W.; Gao, J. Spatial structure of the leisure zone in urban waterfront: A case study of the Grand Canal in downtown Hangzhou. *Geogr. Res.* **2011**, *30*, 1891–1900. (In Chinese)
23. Zheng, L.; Liu, H.; Huang, Y.; Yin, S.; Jin, G. Assessment and analysis of ecosystem services value along the Yangtze River under the background of the Yangtze River protection strategy. *J. Geogr. Sci.* **2020**, *30*, 553–568. [CrossRef]
24. Li, W.; Geng, J.; Bao, J.; Lin, W.; Wu, Z.; Fan, S. Analysis of spatial and temporal variations in ecosystem service functions and drivers in Anxi county based on the InVEST model. *Sustainability* **2023**, *15*, 10153. [CrossRef]
25. Treviño, E.; Hoyos, D.; Sainz de Murieta, E. Economic Valuation of Ocean-Based and Ocean-Related Tourism and Recreation. In *The Blue Economy: An Asian Perspective*; Springer International Publishing: Cham, Switzerland, 2022; pp. 221–243.
26. Wang, R.; Zhao, J.; Chen, G.; Lin, Y.; Yang, A.; Cheng, J. Coupling PLUS–InVEST Model for Ecosystem Service Research in Yunnan Province, China. *Sustainability* **2022**, *15*, 271. [CrossRef]
27. Zhang, W.J.; Sun, X.Y.; Zhou, J. Spatio-temporal dynamics of tradeoffs between crucial ecosystem services in Nansihu Lake Basin. *Acta Ecol. Sin.* **2021**, *41*, 8003–8015.
28. Zhang, Y.; Zhang, B.; Yao, R.; Wang, L. Temporal and spatial changes of vegetation coverage and water production in the Weihe River Basin from 2000 to 2020. *J. Desert Res.* **2022**, *42*, 223–233. (In Chinese)
29. Wu, L.; Fan, F. Assessment of ecosystem services in new perspective: A comprehensive ecosystem service index (CESI) as a proxy to integrate multiple ecosystem services. *Ecol. Indic.* **2022**, *138*, 108800. [CrossRef]
30. Wang, L.; Mao, X.; Song, X.; Tang, W.; Wang, W.; Yu, H.; Deng, Y.; Zhang, Z.; Zhang, Z.; Zhou, H. How rising water levels altered ecosystem provisioning services of the area around Qinghai lake from 2000 to 2020: An InVEST-RF-GTWR combined method. *Land* **2022**, *11*, 1570. [CrossRef]
31. Yang, Q.; Zhang, P.; Qiu, X.; Xu, G.; Chi, J. Spatial-Temporal Variations and Trade-Offs of Ecosystem Services in Anhui Province, China. *Int. J. Environ. Res. Public Health* **2023**, *20*, 855. (In Chinese) [CrossRef] [PubMed]
32. Liu, J.; Yu, B.Y.; Yang, W.F. Evolution mechanism of ecosystem service relationship in the Fenhe River Basin based on multiscale geographically weighted regression. *Natl. Remote Sens. Bull.* **2023**, *27*, 1667–1679. (In Chinese) [CrossRef]
33. Xu, Y.; Song, X.; Deng, M.; Bai, T.; Tao, W. Shifting from Trade-Offs to Synergies in Ecosystem Services Through Effective Ecosystem Management in Arid Areas. *Remote Sens.* **2024**, *16*, 4115. [CrossRef]
34. Qu, Y.; Gong, H.; Zheng, Y.; Shi, J.; Zeng, X.; Yang, H.; Wang, J.; Niu, Z.; Li, L.; Wang, S.; et al. Global conservation priorities for wetlands and setting post-2025 targets. *Commun. Earth Environ.* **2024**, *5*, 4. [CrossRef]
35. Wang, J.G.; Lu, Z.P. A historic review of world urban waterfront development. *City Plan. Rev.* **2001**, *25*, 41–46. (In Chinese)
36. Zhang, B.; Xiong, W.; Ma, M.; Wang, M.; Wang, D.; Huang, X.; Yu, L.; Zhang, Q.; Lu, H.; Hong, D.; et al. Super-resolution reconstruction of a 3 arc-second global DEM dataset. *Sci. Bull.* **2022**, *67*, 2526–2530. [CrossRef]
37. Store, C.C.D. *Land Cover Classification Gridded Maps from 1992 to Present Derived from Satellite Observations*; Copernicus Climate Change Service: Reading, UK, 2019; pp. 7–9.
38. Harris, I.; Osborn, T.J.; Jones, P.; Lister, D. Version 4 of the CRU TS monthly high-resolution gridded multivariate climate dataset. *Sci. Data* **2020**, *7*, 109. [CrossRef]
39. Zheng, C.; Jia, L.; Hu, G. Global land surface evapotranspiration monitoring by ETMonitor model driven by multi-source satellite earth observations. *J. Hydrol.* **2022**, *613*, 128444. [CrossRef]
40. Fischer, G.; Nachtergaele, F.; Prieler, S.; van Velthuizen, H.T.; Verelst, L.; Wiberg, D. *Global Agro-Ecological Zones Assessment for Agriculture (GAEZ 2008)*; IIASA: Laxenburg, Austria; FAO: Rome, Italy, 2008.
41. Ren, D.F.; Qiu, A.Y.; Cao, A.H.; Zhang, W.Z.; Xu, M.W. Spatial responses of ecosystem service trade-offs and synergies to impact factors in Liaoning province. *Environ. Manag.* **2023**, 1–13. [CrossRef] [PubMed]
42. Zheng, Y.; Liu, Y.; Yao, P.; Xie, X.; Zhang, G.; Deng, C. Spatial and temporal changes and prediction of habitat quality in key ecological function area of Hu'nan province. *Bull. Soil Water Conserv.* **2022**, *42*, 347–356, 364. (In Chinese)
43. Deng, X.; Xiong, K.; Yu, Y.; Zhang, S.; Kong, L.; Zhang, Y. A review of ecosystem service trade-offs/synergies: Enlightenment for the optimization of forest ecosystem functions in karst desertification control. *Forests* **2023**, *14*, 88. [CrossRef]
44. Lyu, F.; Tang, J.; Olhnuud, A.; Hao, F.; Gong, C. The impact of large-scale ecological restoration projects on trade-offs/synergies and clusters of ecosystem services. *J. Environ. Manag.* **2024**, *365*, 121591. [CrossRef] [PubMed]
45. Schmitt, T.M.; Haensel, M.; Kaim, A.; Lee, H.; Reinermann, S.; Koellner, T. Recreation and its synergies and trade-offs with other ecosystem services of Alpine and pre-Alpine grasslands. *Reg. Environ. Change* **2024**, *24*, 57. [CrossRef]
46. Pellowe, K.E.; Meacham, M.; Peterson, G.D.; Lade, S.J. Global analysis of reef ecosystem services reveals synergies, trade-offs and bundles. *Ecosyst. Serv.* **2023**, *63*, 101545. [CrossRef]
47. Zeng, M.X.; Lin, S.Q.; Zhang, D.S. Analysis of factors influencing waterfront holiday vitality based on spatial function. In Proceedings of the Chinese society of Landscape Architecture 2020 Annual Conference Proceedings (Volume I), Online, 12–13 December 2020; pp. 219–225. (In Chinese)

48. Luo, R.; Yang, S.; Wang, Z.; Zhang, T.; Gao, P. Impact and trade off analysis of land use change on spatial pattern of ecosystem services in Chishui River Basin. *Environ. Sci. Pollut. Res.* **2022**, *29*, 20234–20248. [CrossRef]
49. Xu, C.; Jiang, Y.; Su, Z.; Liu, Y.; Lyu, J. Assessing the impacts of Grain-for-Green Programme on ecosystem services in Jinghe River basin, China. *Ecol. Indic.* **2022**, *137*, 108757. [CrossRef]
50. Abera, W.; Tamene, L.; Kassawmar, T.; Mulatu, K.; Kassa, H.; Verchot, L.; Quintero, M. Impacts of land use and land cover dynamics on ecosystem services in the Yayo coffee forest biosphere reserve, southwestern Ethiopia. *Ecosyst. Serv.* **2021**, *50*, 101338. [CrossRef]
51. Wu, J.; Li, J.; Ma, Y. Exploring the relationship between potential and actual of urban waterfront spaces in Wuhan based on social networks. *Sustainability* **2019**, *11*, 3298. [CrossRef]
52. Yu, G.; Zhong, S. Borrowed production: Spatial processes of urban waterfront tourism in Guangzhou. *J. Tour. Cult. Chang.* **2022**, *20*, 601–616. [CrossRef]
53. Schulz, T.; Ohmura, T.; Zabel, A. Sustainable economy trade-offs and conflicts in and with the forest (Research Trend). *For. Policy Econ.* **2023**, *150*, 102936. [CrossRef]

Disclaimer/Publisher's Note: The statements, opinions and data contained in all publications are solely those of the individual author(s) and contributor(s) and not of MDPI and/or the editor(s). MDPI and/or the editor(s) disclaim responsibility for any injury to people or property resulting from any ideas, methods, instructions or products referred to in the content.